

2010

# The Impact of Exterior Overhangs on the Daylighting Performance of Office Spaces

Sagar Rao  
*Purdue University*

Athanasios Tzempelikos  
*Purdue University*

Follow this and additional works at: <http://docs.lib.purdue.edu/ihpbc>

---

Rao, Sagar and Tzempelikos, Athanasios, "The Impact of Exterior Overhangs on the Daylighting Performance of Office Spaces" (2010). *International High Performance Buildings Conference*. Paper 33.  
<http://docs.lib.purdue.edu/ihpbc/33>

This document has been made available through Purdue e-Pubs, a service of the Purdue University Libraries. Please contact [epubs@purdue.edu](mailto:epubs@purdue.edu) for additional information.

Complete proceedings may be acquired in print and on CD-ROM directly from the Ray W. Herrick Laboratories at <https://engineering.purdue.edu/Herrick/Events/orderlit.html>

# The Impact of Exterior Overhangs on the Daylighting Performance of Office Spaces

Sagar RAO<sup>1</sup>, Athanasios TZEMPELIKOS<sup>2\*</sup>

<sup>1</sup> School of Civil Engineering, Purdue University, West Lafayette, Indiana, USA  
E-mail: raos@purdue.edu

<sup>2</sup> School of Civil Engineering, Purdue University, West Lafayette, Indiana, USA  
Tel.: 765-496-7586, E-mail: ttzempel@purdue.edu

\* Corresponding Author

## ABSTRACT

This paper presents a simulation study about the daylighting performance of exterior overhangs. Overhangs are passive shading systems that are used to exclude solar gains in summer and allow some solar heat in the winter, while they can partly protect from glare and still allow view to the outside. The impact of overhang characteristics (width, reflectance and geometry) on the indoor illuminance levels and projected sunlit area on the floor was studied for a private office in Lafayette, IN. The window was split in three parts, depending on the relative position of the overhang and solar angles, in order to calculate shaded and unshaded window areas for every hour in the year. Then a multiple-bounce radiosity method was utilized to predict work plane illuminance on a surface grid and within the time-varying 10-surface enclosure. Annual daylight autonomy and fractions of shaded windows and sunlit floor areas were computed as a function of overhang geometry and reflectance throughout the year.

## 1. INTRODUCTION

Buildings in the US account for about thirty percent of the total primary energy consumption (and associated GHG emissions) and about one third of this energy is used for lighting (EIA, 2003). Most commercial establishments operate during the day, when natural light can substitute (or at least supplement) artificial lighting, resulting in significant energy savings (Tzempelikos and Athienitis, 2007, Ihm *et al.*, 2009, Krafti *et al.*, 2005). However, solar protection is necessary in order to protect from glare and overheating. External shading is more effective than internal, since solar gains are efficiently rejected. External shading devices are also preferred over low transmittance glazing, because they have a smaller effect on outdoor view and can be dynamically operated.

Passive exterior shading devices are still able to perform well: an external overhang reflects a significant amount of daylight through the auxiliary aperture, which contributes in uniform interior illuminance distributions and enhances the perception of openness associated with it (Claros and Soler, 2001, Ochoa and Capeluto, 2006, Refaie, 1987). Moreover, overhangs reduce overheating and cooling load during summer months at a time of the day when electricity is most expensive. During winter, they allow some solar heat which can be desirable in cold climates (Dubios, 1998, 1999).

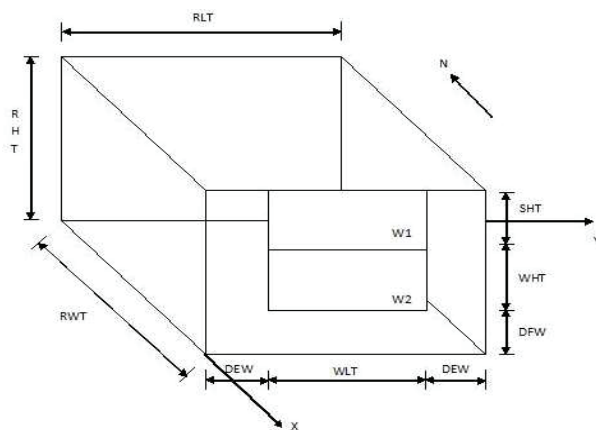
However, inappropriate use of shading devices can result in problems such as excessive glare and visual discomfort and limited view to the outside, both of which are unfavorable. Therefore, an appropriate external overhang is one that enhances indoor illuminance levels without causing significant glare during most of the working hours (Abdulnohsen *et al.*, 1994, Tavares *et al.*, 2006). It should also provide maximum possible view of the exterior, and at the same time achieve acceptable energy performance (Raeissi and Taheri, 1998, Schuster, 2006, Janak, 2003). With this discussion, it may be concluded that the performance of an overhang can be completely understood by studying the physical characteristics of the device (geometry, position, reflectance) and its ability to (i) reduce glare (ii) improve illuminance distribution and (iii) reduce energy use for lighting and air-conditioning. This study aims to assess these performance parameters for an overhang shading a private office with one exterior wall (window) in order to help designers select and optimize such devices.

## 2. CALCULATION METHOD

### 2.1 Model Details and Problem Definition

The analysis was performed for a private office in Lafayette, IN. 46% of the south-facing façade is occupied by windows. The simulation considers that daylight is the lone source of illumination in the space. The inner surfaces are a generic representation, whose properties are defined in terms of their reflectances. The window (see Figure 1) is divided into two separate sections;  $W1$  (top portion; auxiliary aperture) and  $W2$  (bottom portion; view aperture). The overhang is a 2-D horizontal plane that merely splits the large window, thus reflecting solar beam radiation incident on it to  $W1$  while shading  $W2$ . The window is double glazed with a standard thickness and extinction coefficient (details described below).

The model is versatile since all basic simulation parameters (model inputs) are variables: room location, space dimensions, window size, overhang specifications, orientation of the façade, enclosure surface properties, etc. and may be altered at any time. However, two conditions must be met at all times for ease of calculations: (i) the window sill is at the work plane height and (ii) the window is located at the centre of the façade.



RHT = ROOM HEIGHT = 3m  
 RWT = ROOM WIDTH = 4 m  
 RLT = ROOM LENGTH = 4 m  
 WHT = WINDOW2 HEIGHT = 1.2 m  
 WLT = WINDOW2 LENGTH = 2.5 m  
 SHT = WINDOW1 HEIGHT = 1 m  
 SWT = OVERHANG LENGTH = 0.25 m to 1 m  
 WINDOW PANE THICKNESS = 6 mm  
 $k$  = EXTINCTION COEFFICIENT =  $7.76 \text{ m}^{-1}$   
 GROUND REFLECTANCE = 20%  
 CEILING REFLECTANCE = 80%  
 WALL REFLECTANCE = 70%  
 FLOOR REFLECTANCE = 40%  
 SPECULAR SHELF REFLECTANCE = 50%-90%

Figure 1: Model geometry and input parameters.

### 2.2 Surface Calculations and View Factors

It may be observed that, depending on the position of the sun, and the orientation of the façade (with respect to the geographic poles), for a given overhang geometry and position,  $W2$  can be completely shaded, partially shaded, or not shaded at all. This, in turn, decides if direct light enters the space through the view aperture. Hence, it becomes increasingly important to compute the percentage area of  $W2$  that is unshaded (on a given day and time), as a function of the overhang length. Here, however, an assumption is made that the unshaded portion of the window is a rectangle of the same length as the window, whose height is determined by the projection of the overhang at that instant, i.e. it is a function of day number ( $n$ ) and standard time ( $t_{STD}$ ).

Exposure of the view aperture to direct light results in beam radiation transmitted through the glass, which in turn is incident on a specific portion of the floor. The model computes the hourly exact position of the sunlit floor area (window projection) throughout the year. For this purpose, the floor plan (work plane) was segmented into a grid, where each point on it was completely defined by means of a 2D Cartesian coordinate system. The exact coordinates of the projection were found using a single-bounce ray-tracing calculation, in terms of the altitude angle ( $\alpha$ ) and solar azimuth angle ( $\psi_s$ ); both of which are again functions of  $n$  and  $t_{STD}$ . A schematic of window projection and related dimensions are shown in Figure 2. The coordinates of the sunlit area are calculated from Equation (1).

Since the projected area changes with time and day, a dynamic module was developed to compute the time-varying view factors between all interior surfaces using fundamental geometrical equations (Siegel and Howell, 1972). An important part of this model is how it treats the different (variable) surfaces in the radiosity calculations that follow. At a given time, depending on whether one (single window), two ( $W1$  and completely shaded  $W2$ ), three ( $W1$ , shaded  $W2$  and non-shaded  $W2$ ) or four ( $W1$ , shaded  $W2$ , non-shaded  $W2$  and sunlit floor area) distinct initial luminous sources exist, the room is treated as a 7-, 8-, 9- or 10-surface enclosure respectively, with significant computational effort required for the last two cases.

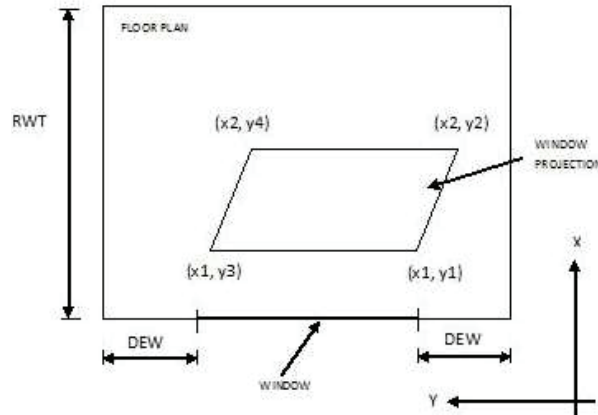


Figure 2: Window projection on the floor and vertex coordinates.

$$\begin{bmatrix} x_1 = \frac{DFW}{\tan(\alpha)} \\ x_2 = \frac{DFW + H_{unshaded}}{\tan(\alpha)} \\ y_1 = x_1 \cdot \tan(\Psi_s) + DEW \\ y_2 = x_2 \cdot \tan(\Psi_s) + DEW \end{bmatrix} \quad (1)$$

### 2.3 Incident Exterior Illuminance

Solar geometry calculations are first performed to calculate hourly solar incidence angles. Hourly weather data for the year was then obtained from the Typical Meteorological Year (TMY3) weather database. Considering the sky to be an anisotropic source of diffuse light, the Perez et al. (1990) all-weather sky model was used to calculate the hourly sky diffuse illuminance on the façade. The basic input parameters from the hourly TMY data are: direct normal illuminance ( $DNE$ ), diffuse horizontal illuminance ( $DHE$ ) and the extraterrestrial normal irradiance ( $ETRN$ ). The amount of incident illuminance on each of the window surfaces (resulting from the shading pattern) was then computed. A different amount of light is incident on the two portions (shaded and unshaded) of the bottom window. Therefore, the amount of daylight incident on three portions of the window namely;  $W1$ ,  $W_{shaded}$  and  $W_{unshaded}$  was calculated as follows.

- For the upper window ( $W1$ ):

$$E_l = E_{beam} + E_{d,sky} + E_{over} + E_{d,ground} \cdot \left( \frac{\xi_l}{90^\circ} \right) \quad (2)$$

where  $E_{beam}$  is the direct illuminance from the sun,  $E_{d,sky}$  is the incident diffuse illuminance from the sky and  $E_{d,ground}$  is the fraction of horizontal (ground) illuminance reaching the vertical window surface, given by:

$$E_{d,ground} = (DHE + DNE \cdot \sin(\alpha)) \cdot \rho_g \cdot \frac{1 - \cos(\beta)}{2} \quad (3)$$

where  $\alpha$  is the solar altitude,  $\beta$  is the slope of the surface (window =  $90^\circ$ ) and  $\rho_g$  is the ground reflectance. The angle  $\xi_l$  is a compensation factor which accounts for the fact that the window does not see the part of the ground that is close to the façade (Figure 3). It is equal to:

$$\tan(\xi_l) = \frac{SHT}{2L} \quad (4)$$

where  $SHT$  is the height of the upper window and  $L$  is the overhang width.

- For the overhang upper surface:

$$E_{over} = (DHE + E_{beam}) \cdot \rho_{over} \cdot F_{over,wl} \quad (5)$$

where  $\rho_{over}$  is the overhang reflectance and  $F_{over,wl}$  is the view factor from the overhang to the upper window section.

- For the shaded and unshaded portion of the lower window, respectively:

$$E_{shaded} = E_{d,ground} + E_{d,sky} \cdot \left( \frac{\xi_2}{90^\circ} \right) \quad (6)$$

$$E_{unshaded} = E_{beam} + E_{d,ground} + E_{d,sky} \cdot \left( \frac{\xi_2}{90^\circ} \right) \quad (7)$$

where the angle  $\xi_2$ , similar to  $\xi_1$ , is a compensation factor necessary since the shaded portion is unable to see all of the sky (Figure 3). It may be calculated from:

$$\tan(\xi_2) = \frac{L}{H_{shaded}} \quad (8)$$

where  $H_{shaded}$  is the part of the lower window that is shaded by the overhang (Fig. 3), equal to:

$$H_{shaded} = L \cdot \tan(\alpha) \quad (9)$$

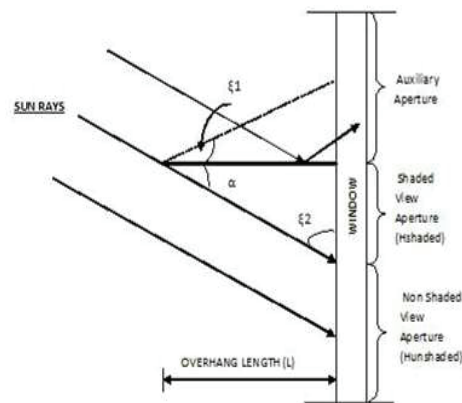


Figure 3: Façade surfaces used for incident illuminance and view factors calculations and related angles.

## 2.4 Window Optics and Radiosity Method

The model considers a double glazed window (Double Strength A-Quality glass with a thickness of 6 mm and an extinction coefficient of  $7.76 \text{ m}^{-1}$ ). Using standard optics calculations (ASHRAE, 2009), the beam transmittance ( $\tau_{beam}$ ) of the window was obtained as a function of solar incidence angle, i.e., for every hour the year. With the window transmittances and the incident illuminances known, the hourly initial luminous exitance of every window surface was found. Then, using the radiosity method, the final exitance of all the pertinent surfaces ( $M_1, M_2 \dots M_{10}$ ) after infinite inter-reflections was computed throughout the year using the following formula (Murdoch, 2003):

$$M_n = M_{on} + \rho_n \sum_{m=1}^{10} M_m \cdot F_{mn} \quad (10)$$

where  $M_{on}$  is the initial luminous exitance of surface  $n$ ,  $\rho_n$  is the reflectance of surface  $n$  and  $F_{mn}$  is the view factor from surface  $m$  to surface  $n$  respectively. The initial luminous exitance of all the surfaces except the window surfaces and the sunlit floor area (if it does exist) are equal to zero. For calculation of work plane illuminance, a grid of nine points was selected and the configuration factors from each of the surfaces to the nine points on the grid were computed. The illuminance on the work plane surface grid (point  $p$ ) was thus calculated using the formula:

$$E_p = \sum_{n=1}^{10} C_{pn} M_n \quad (11)$$

where  $C_{pn}$  is the configuration factor from point  $p$  to surface  $n$  (Murdoch, 2003).

### 2.5 Average Daylight Autonomy, Energy Savings and Cost Benefits

With the illuminance at the nine points defined as a function of solar time, the calculations were performed for each hour of the year. Daylight autonomy ( $DA$ ), an annual measure of how often a minimum work plane illuminance requirement of 500lx (typical set point) can be met by daylight alone (Reinhart et al., 2006, Nabil and Mardaljevic, 2006) is calculated for the work plane grid for all working hours in the year (9am-6pm). The average daylight autonomy ( $ADA$ ) was calculated as the average of the nine  $DA$  values (points). The resulting energy savings and cost benefits were calculated using the formula (Tzempelikos and Athienitis, 2007):

$$S = P_L \cdot t_y \cdot A \cdot ADA \quad (12)$$

where  $P_L$  is the lighting power density,  $A$  is the floor surface area and  $t_y$  is the amount of working hours in the year. In this simulation, the above parameters were equal to:  $P_L=12\text{W/m}^2$ ,  $A = 16 \text{ m}^2$  and  $t_y=2349$  hrs (excluding nights and weekends). The cost savings are then easily calculated by multiplying the energy savings by the cost of electricity.

## 3. SIMULATION RESULTS

### 3.1 Fraction of lower window not shaded by overhang

The following plots show the percentage area of the lower window ( $W_2$ ) that is unshaded for two representative days in winter and summer (February 3<sup>rd</sup> and June 29<sup>th</sup>) using different overhang widths. During the summer, for a small overhang of about 0.25m, at least 30% of the window remains unshaded when sunlight is incident on it. The percentage shaded area increases with a larger overhang, and for an overhang 1m wide, the window can be completely shaded between 12-2 pm. In winter, given that the sun is lower in the sky, only a small portion the window is shaded. With the largest overhang (1m), the shaded area is maximum (about 55%) around 1 pm. However, at the beginning and at the end of the day, almost the entire window remains unshaded, which will result in significant glare problems.

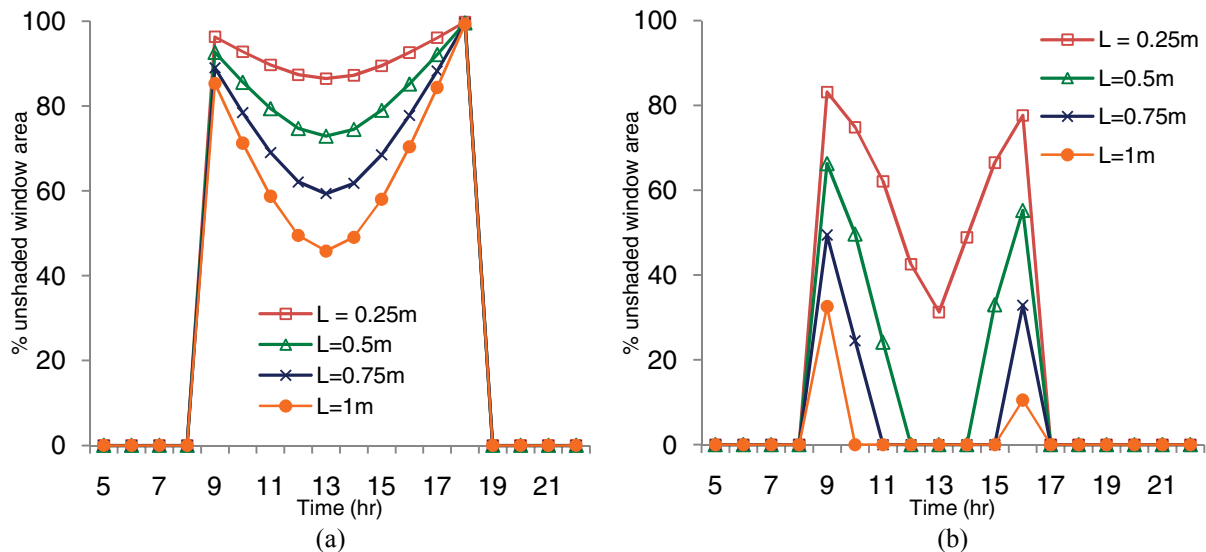


Figure 4: Fraction of unshaded window area for representative days in (a) winter and (b) summer with different overhang widths.

### 3.2 Sunlit Floor Area (SFA)

Figures 5(a) and 5(b) present the fraction of floor area that receives direct sunlight (SFA%) during the same representative days as for Fig. 4. It is clearly seen that, the smaller the overhang, the larger the window projection on the floor. In winter, the directly illuminated areas are considerably high, and for an overhang length of 0.25m up to 30% of the floor may receive beam radiation. Even with a large (1m) overhang, complete shading of the floor is not accomplished. In the summer, for a sufficiently large overhang (1m), the floor is never exposed to beam radiation

(complete shading from direct sunlight is achieved). For a smaller overhang (0.25m), however, upto 6% of the floor may experience direct light.

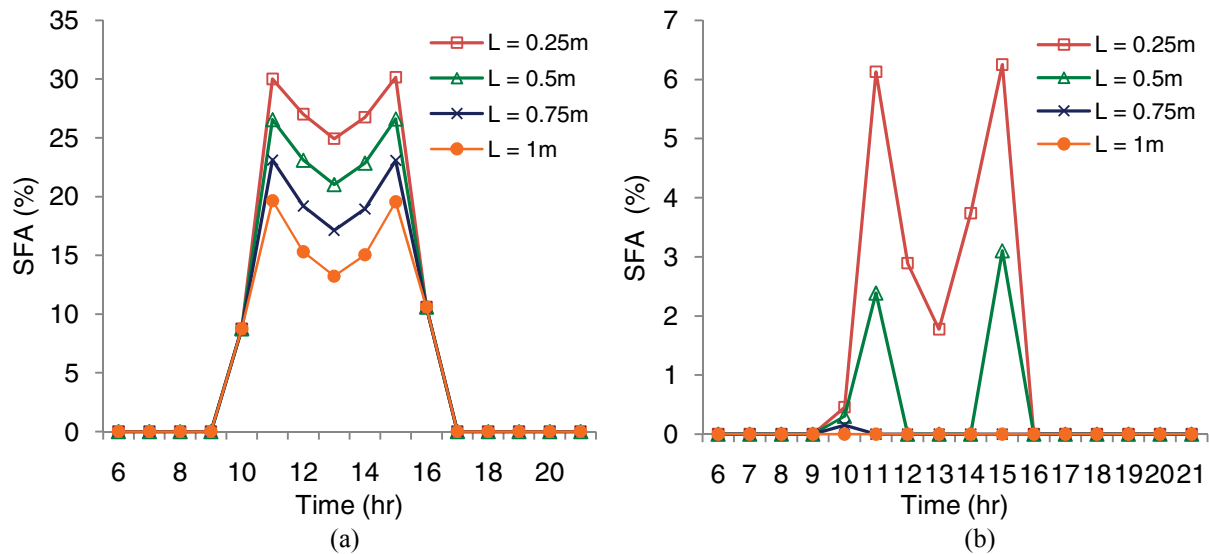


Figure 5: Percent sunlit floor area for representative days in (a) winter and (b) summer with different overhang widths.

The exact coordinates of the window projection on the floor are calculated for every hour in the year. Figures 6(a) and 6(b) show the fraction of sunlit floor area for every working hour in the year, for two overhang widths: 0.25m and 1m. As expected, the values are maximized in the winter and during daytime. These results indicate the risk and frequency of glare potential for the different cases.

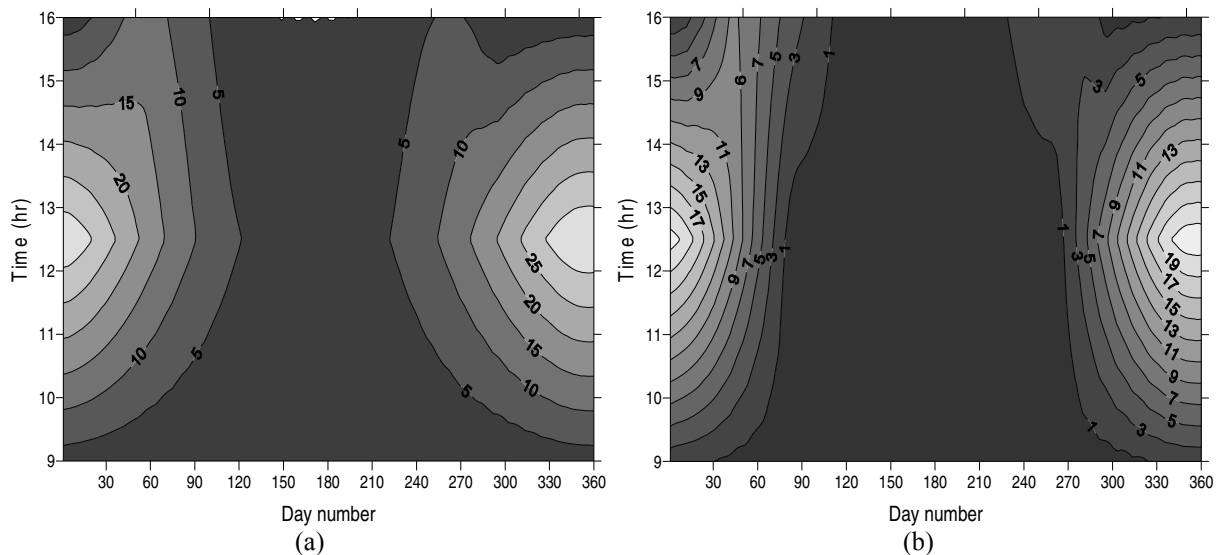


Figure 6: Fractions of sunlit floor area throughout the year for overhang widths (a) 0.25m and (b) 1m.

### 3.3 Illuminance Distributions

Figures 7(a) and 7(b) illustrate the change in illuminance along the center of the room at specific distances from the window, at noon, on February 3<sup>rd</sup> and June 29<sup>th</sup> respectively. In the summer, for a 0.25m overhang, the area close to the window (within 0.5m from it) receives direct light. The illuminance levels through rest of the room are considerably smaller. It should be noted that, since the room is not very deep, the effect of the larger source area (unshaded portion of  $W/2$ ) has a more significant effect on the Illuminance distribution and hence a smaller overhang provides higher illuminance within the space. However, glare issues arising from smaller overhangs cannot be

neglected. With a large overhang (1m) sufficient shading can be achieved. For a winter day, a larger section of the floor receives direct light. Nevertheless, larger overhangs result in lesser *SFA* (as discussed in the previous section) with a narrower shaft of light falling on the floor.

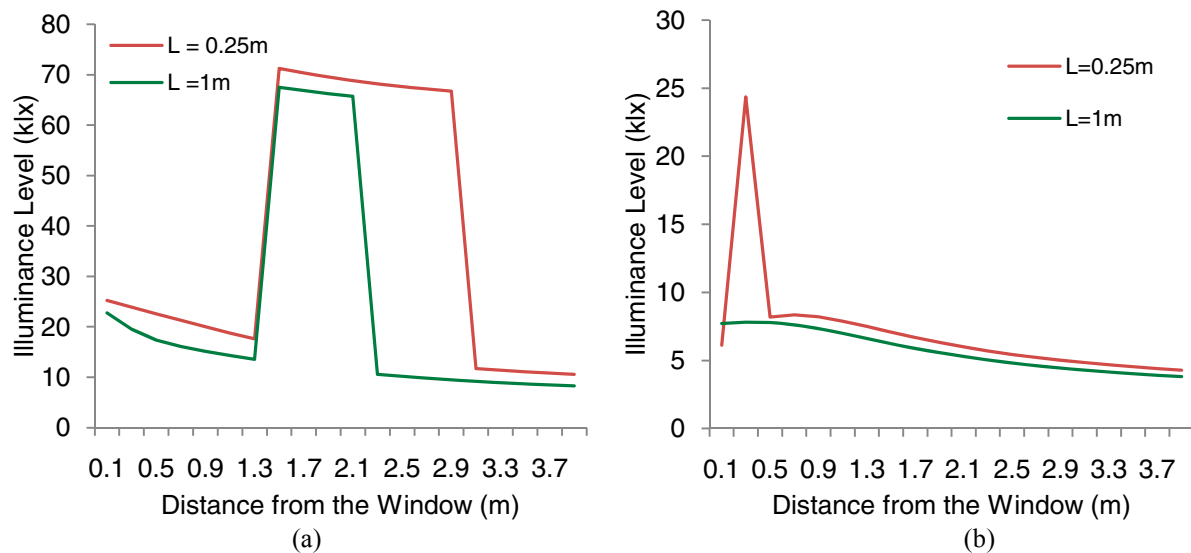


Figure 7: Work plane illuminance distribution for for representative days in (a) winter and (b) summer with different overhang widths.

### 3.4 Variation of Average Daylight Autonomy with overhang width and reflectance

Figure 8 presents the calculated *ADA* for various overhang dimensions and reflectance combinations. High reflectance results in higher daylight autonomy for a given width. The differences are small due to the small size of the room. The impact of overhang width is more evident for higher reflectance values. For the same reflectance value, a smaller overhang provides higher illuminance. However, for a deeper room, one would expect that these results would change to reflect the impact of light redirection on the ceiling with improved uniformity in the light distribution.

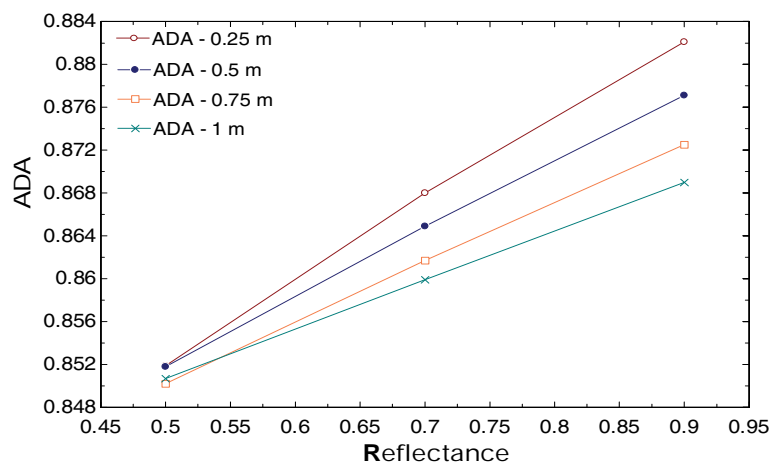


Figure 8: Average Daylight Autonomy as a function of overhang width and reflectance for the studied room.

## 4. CONCLUSIONS

This paper studied the impact of overhang characteristics (width, reflectance and geometry) on the indoor illuminance levels and projected sunlit area on the floor was studied for a private office in Lafayette, IN. An

important part of this flexible model is how it treats the different (variable) surfaces in the radiosity calculations. The window was split in three parts, depending on the relative position of the overhang and solar angles, in order to calculate shaded and unshaded window areas for every hour in the year. Then a multiple-bounce radiosity method was utilized to predict work plane illuminance on a surface grid and within the time-varying 10-surface enclosure. Annual daylight autonomy and fractions of shaded windows and sunlit floor areas were quantified as a function of overhang geometry and reflectance throughout the year. Direct sunlight will create glare problems for variable amounts of hours (depending on overhang geometrical characteristics) and therefore a combination of an overhang with other shading devices is recommended. This work will be extended to include several room geometries and climatic locations.

## REFERENCES

- Abdulnohsen A., Boyer L.L., Degelman L.O., 1994, Evaluation Of Light-shelf Daylighting Systems for Office Buildings in Hot Climates, In: *Proceedings of 9<sup>th</sup> Symposium on Improving Building Systems in Hot and Humid Climates*, USA.
- American Society of Heating, Refrigeration and Air-Conditioning, 2009, *ASHRAE Handbook-Fundamentals*, Atlanta, USA.
- Claros T.S., Soler A., 2001, Indoor Daylight Climate-Comparison Between Light Shelves and Overhang Performances in Madrid For Hours with Unit Sunshine Fraction And Realistic Values Of Model Reflectance, *Solar Energy*, Vol.71, no.4, p: 233–239.
- Dubios M.C., 1998, Awnings and Solar-Protective Glazing for Efficient Energy Use in Cold Climates, In: *Proceedings of Renewable Energy technologies in Cold Countries, Montreal (Canada)*, p: 380–385.
- Dubios M.C., 1999, The design of seasonal awnings for low cooling and heating loads in offices, In: *Proceedings of 5<sup>th</sup> Symposium on Building Physics in the Nordic Countries, Goteborg, Sweden*, p: 505–512.  
[http://www.eia.doe.gov/emeu/cbecs/cbecs2003/detailed\\_tables\\_2003/detailed\\_tables\\_2003.html](http://www.eia.doe.gov/emeu/cbecs/cbecs2003/detailed_tables_2003/detailed_tables_2003.html)
- Ihm P., Nemri A., Krarti M., 2009, Estimation of lighting energy savings from daylighting, *Building and Environment*, Vol. 44, no 36, p: 509–514.
- Janak M., 2003, Whole Building Energy Simulation with Complex External Shading Devices, In: *Proceedings of Eighth International IBPSA Conference, Netherlands*.
- Krarti M., Erickson P. M., Hillman T. C., 2005, A simplified method to estimate energy savings of artificial lighting use from daylighting, *Building and Environment*, Vol. 40, no 6, p: 747–754.
- Murdoch J., 2003, *Illuminating Engineering from Edison's Lamp to the LED*, Visions Communications, New York, USA, Pages 750.
- Nabil, A., Mardaljevic, J., 2006, Useful daylight illuminances: a replacement for daylight factors, *Energy and Buildings*, vol. 38: p. 905-913.
- Ochoa C.E., Capeluto I.G., 2006, Evaluating visual comfort and performance of three natural lighting systems for deep office buildings in highly luminous climates, *Building and Environment*, Vol. 41, no 8, p: 1128–1135.
- Perez R., Ineichen P., Seals R., Michalsky J., Stewart R., 1990, Modeling Daylight Availability and Irradiance Components from Direct and Global Irradiance, *Solar Energy*, Vol. 44, no. 5, p: 27–289.
- Raeissi S., Taheri M., 1998, Optimum Overhang Dimensions for Energy Saving, *Building and Environment*, Vol. 33, no. 5, p: 293–302.
- Refaie M.F., 1987, Performance Analysis of External Shading Devices, *Building and Environment*, Vol. 22, no. 4, p: 269–284.
- Reinhart, C., Mardaljevic, J., Rogers, Z., 2006, Dynamic daylight performance metrics for sustainable building design, *Leukos*, vol. 3, no.1: p. 1-25.
- Schuster H.G., 2006, The influence of Daylight Design in Office Buildings on the User Comfort, In: *Proceedings of 23<sup>rd</sup> Conference on Passive and Low Energy Architecture, Switzerland*, PLEA2006.
- Siegel R., Howell J., 1972, Radiation Heat Exchange in an Enclosure Composed of Diffuse- Gray Bodies, *Thermal Radiation Heat Transfer*, McGraw Hill Book Company, USA, Pages 814.
- Tavares S. G., Kinsel S. L., da Costa Silva H., 2006, Parametric Lighting Studies, *The 23<sup>rd</sup> Conference on Passive and Low Energy Architecture, Switzerland*.
- Tzempelikos, A., Athienitis, A.K., 2007, The impact of shading design and control on building cooling and lighting demand, *Solar Energy*, vol. 81: p. 369-382.
- US Energy Information Administration, 2003.